TIME-DOMAIN IMPLEMENTATION OF SOIL-STRUCTURE INTERACTION ANALYSIS TECHNIQUES WITH FREQUENCY-DEPENDENT IMPEDANCE FUNCTIONS

IMPLÉMENTATION DES TECHNIQUES D'ANALYSE DE L'INTERACTION SOL-STRUCTURE DANS LE DOMAINE TEMPOREL AVEC DES FONCTIONS D'IMPÉDANCE DÉPENDANTES DE LA FRÉQUENCE

Réception : 23/04/2023 Acceptation : 17/05/2023 Publication : 20/06/2023

BENCHARIF Raouf [1], ZAHAFI Amina[2], MEZOUAR Nourredine[3], HADID Mohamed[4]

[1]Centre National de Recherche Appliquée en Génie Parasismique, CGS, Hussein Dey, Alger, Algérie-rbencharif@cgs-dz.org
[2]Ecole Nationale Supérieure des Travaux Publics (ENSTP), Kouba, Alger, Algérie-amina_zahafi@yahoo.com
[3]Centre National de Recherche Appliquée en Génie Parasismique, CGS, Hussein Dey, Alger, Algérie-nmezouar@cgs-dz.org
[4]Ecole Nationale Supérieure des Travaux Publics (ENSTP), Kouba, Alger, Algérie-hadid_mohamed2003@yahoo.fr

Abstract- Engineers commonly use the substructure method to account for soil-structure interaction (SSI) in the seismic design of structures. This method distinguishes between two components of SSI: kinematic and inertial interaction. Inertial interaction requires modeling the foundation-soil interface with complex-valued impedance functions that behave like springs and dampers, transferring motion between the soil-foundation system and the far-field. While impedance functions for simple foundation geometries and soil profiles are available in the literature, their frequency dependence makes their use in response history analysis challenging, especially for nonlinear structures. To address this issue, several methods have been proposed, which are reviewed in this paper, including their advantages, disadvantages, and scope of application, along with simple numerical examples of each method's concept.

Keywords: Frequency-Dependent Impedance Function, Time Domain Substructure Method, Hybrid Frequency-Time Domain, Lumped Parameters Model,Recursive Filters Method.

Résumé-Les ingénieurs utilisent couramment la méthode de sous-structure pour prendre en charge l'interaction sol-structure (ISS) dans la conception parasismique des structures. Cette méthode permet de différencier deux composantes distinctes de l'ISS, à savoir l'interaction cinématique et l'interaction inertielle. Pour ce qui est de l'interaction inertielle, la modélisation de l'interface fondation-sol à l'aide de fonctions d'impédance à valeurs complexes est nécessaire. Ces fonctions peuvent être visualisées comme un ensemble de ressorts et d'amortisseurs qui transfèrent le mouvement entre le système sol-fondation et le champ lointain. Des fonctions d'impédance pour des géométries de fondation simples et des profils de sol sont disponibles dans la littérature, tandis que les progrès des méthodes de calcul ont permis de générer de telles fonctions pour des systèmes de fondation-sol plus complexes. Leur dépendance à la fréquence est cependant un obstacle majeur à leur utilisation généralisée, ce qui complique leur utilisation dans les analyses temporelles, en particulier lorsque la super structure présente une non-linéarité. Pour résoudre ce problème, plusieurs méthodes ont été proposées dans l'état de l'art actuel. Cet article vise à passer en revue ces méthodes et à fournir des exemples numériques simples pour faciliter la compréhension de chaque concept. De plus, l'article abordera les avantages, les inconvénients et le champ d'application de chaque méthode.

Mots - clés : Fonction D'impédance Dépendante De La Fréquence, Méthode De Sous-Structure Dans Le Domaine Temporel, Méthode Hybride Fréquence-Temps, Modèle À Paramètres Concentrés, Méthode Des Filtres Récursifs.

1-Introduction

The response of a structure to an earthquake shaking depends on the interactions among the structure, the foundation, and the surrounding geologic media. These interactions cause the stiffness of the soil to be coupled with that of the structure, which modifies the mechanical properties of the system.Kausel[1] defines SSI as an interdisciplinary field that combines soil and structural mechanics, dynamics, earthquake engineering, geophysics, geomechanics, material science, and computational methods. Its origins date back to the late 19th century and have matured over time, progressing rapidly during the second half of the 20th century due to the needs of various industries and advancements in computer technology. On the other hand, Roesset[2]attributes the emergence of the field of structural dynamics as an independent research area to early pioneers such as Sezawa, Martel, and Housner. These pioneers studied seismic events and the resulting structural responses, noting discrepancies between observed responses and contemporary theories that assumed structures moved in exact compliance with their supporting media[3].

The SSI effect can be evaluated by comparing the system's responses with and without SSI. SSI can cause period lengthening and an increase in damping due to soil-structure coupling and radiation effects. The effect of SSI on a structure's demand depends on the change in its fundamental period. When the period elongates due to SSI, the demand decreases, and when it shortens, the demand increases. Zhang and Tang[4]measured these effects using dimensionless analysis and found that the impact of SSI on base shear is related to the slope of the spectrum: positive slope increases base shear, while negative slope decreases it.

While design spectra are useful tools, they only give an estimation of the maximum response parameters. In many cases, designers are more interested in the time history response of a structure. A full-time history gives the structural response over time during loading duration. The time history analysis is very useful tools, particularly for nonlinear systems. To this end, two main categories namely, multistep methods (substructure approach) and direct approach can be used to deal with SSI problem.

The substructure method, which was introduced by Kausel et al.[5], involves three steps for determining the response of a soil-structure interaction system. In the first step, a transfer function is used to calculate the foundation movement and input motion. The second step models the soil as a set of springs and dashpots, known as dynamic impedance functions, to evaluate the inertial interaction effects. In the final step, the previously solved impedance function and kinematic interaction are used to calculate the system response. While the substructure method assumes linear behavior of the soil and structure, recent seismic design requirements have necessitated research into nonlinear behavior. The aim of the paper is to provide an overview of existing procedures for approximating frequency-dependent foundation impedance functions in the time-domain, illustrated through numerical examples.

2- Foundation impedance functions

Foundation impedance functions offer a means of mathematically representing a truncated soil domain’s reaction at the soil-foundation interface. The response of a rigid foundation to static or dynamic external loads results from the deformation of the surrounding and supporting soil. The static soil stiffness is used to idealize the soil-foundation system in order to obtain the response to static loads. In an analogous manner, the dynamic soil impedance/stiffness is used to idealize the soil-foundation in order to obtain the response to dynamic loads. Six components of dynamic impedances are required, 03 translational and 03 rotational, to set up the system of dynamic equations of a rigid foundation. These impedances depend on the foundation geometry, the soil properties and embedment depth.

Several approaches for calculating the dynamic impedance function was developed; these approaches include: (a) Analytical methods [6],[7], [8], (b) Approximate analytical methods[9], (c) Simplified methods also known as strength of material approaches[10], [11], (d) Computer-based numerical methods such as Finite Element Methods[12], Boundary Element Methods[13], and hybrid techniques[14],[15],

[16].Compreh-ensive literature reviews of the available methods have been conducted by Bencharif[17].

While specific notation tends to vary, foundation impedance functions typically take the following form[6]

$$\bar{k}_j = k_j(\omega) + \mathrm{i}\omega c_j(\omega) \quad (1)$$

where k_j represents stiffness, c_j represents damping, the subscript j represents the direction of motion, and i represents$\sqrt{-1}$. In addition to the linear frequency dependence inherent in the imaginary term, both k_j and c_j may also vary with frequency (ω). Thus, an alternative form for of Eq. (1)is

$$\bar{k}_j = k_j(1 + 2i\beta_j) \quad (2)$$

$$\beta_j = \frac{\omega c_j}{2k_j} \quad (3)$$

An advantage of using β_j over c_j is that at resonance of the SSI system, $\beta_j$is interpreted as a percentage of critical damping in the classical sense[18].

3- The substructure method: time history analysis

After determining the input motion and foundation impedance functions for a soil-foundation-structure system, the final step in the substructure method involves calculating the expected response of the structure. Impedance functions usually exhibit frequency-dependent characteristics, including a cut-off frequency with negligible damping below and rapid damping increase above, slight, or significant oscillations in the impedance function of a surface or embedded rigid foundation depending on soil homogeneity and bedrock depth, and multiple oscillations in pile groups. To perform a dynamic linear or nonlinear time-history analysis, several methods based on time-domain transformations of frequency-dependent dynamic impedance functions have been proposed and available in the literature for years. Among the most famous methods in the literature are:

1. *Frequency domain solution:* The nuclear industry uses the frequency domain analysis method for SSI analysis, assuming soil and structures to be equivalent-linear or linear elastic materials, as nuclear facilities are designed to behave near the elastic range during a design-level earthquake (Laudon et al.[19]). The governing equations of motion are solved in frequency domain using a structure's transfer function, which is a function of frequency and can easily deal with frequency-dependent foundation impedance functions. However, this method is only suitable for linear analyses and cannot be used for structures experiencing inelastic deformations.

2. *Representative frequency solution*: This method removes frequency dependence from impedance functions by evaluating them at a representative frequency. The frequency can be the flexible-base first mode natural frequency of the structure or the frequency of a representative single-degree-of-freedom system. This method works well for elastic structures with responses dominated by the first mode. However, inelastic structures with changing natural frequency during excitation or those with a "serrated" impedance function showing significant frequency variation may encounter issues. This is commonly seen in multilayered soil on rigid bedrock or layered systems with large layer contrasts (Ghannad et al.[20]; NIST GCR 12-197-21[21]).

3. *The Lumped Parameter Model (LPM):*this method consists of replacing foundation impedance functions with sets of masses, dashpots, and springs, and has two simple model types: the standard and fundamental models. The standard model uses spring stiffness K and curve-fitting parameters C and M, while the fundamental model has one static stiffness parameter and four curve-fitting parameters. LPMs are advantageous because they can be easily incorporated into conventional software and applied to non-linear superstructures using time stepping methods such as Newmark's method. References include Wolf [10], Wu et al.[22] and recently Zahafi et al. [23], [24].

4. The convolution-based solution,sometimes called hybrid frequency-time domain method, transforms impedance functions into an impulse response in the time domain, with origins dating back to Wolf and

Obernhuber[25]. Since then, researchers have proposed and improved various versions, such as those by Wolf and Motosaka[26], Meek[27], Motosaka and Nagano[28], Hayashi and Katsukura[29], and Nakamura[30], [31], [32], [33]. This method has potential to account for inelastic structural deformations but has significant computational expense and accuracy issues due to time-domain leakage, as discussed by Gash [3].

5. The discrete-time filter method represents soil-foundation system reaction force as a function of the previous time step's state variables. Wolf and Motosaka[26] proposed rational approximations of frequency-dependent impedance functions that can be applied recursively, while Paronesso and Wolf [34] offered further details on their determination. Ruge et al. [35]proposed an alternative multivariable approach, and Du and Zhao [36] added a stability condition. Şafak[37] proposed using signal processing theory to approximate impedance functions as discrete-time digital filters in time domain analyses, generating reaction forces dependent on previous time steps and foundation displacement time history.

4- Implementation of existing methods

This section examines the basic soil-structure system shown in Figure 1 comprising a single degree-of-freedom and a rigid disk on a uniform half-space. Table 1 displays the properties of the half-space. The input base excitation for the fixed base structure and soil structure system will be the North-South surface motion recorded at JMA survey station during the January 17th, 1995, Kobe Earthquake. The acceleration record for this event contains $L = 2000$ data points spaced at $\Delta t = 0.02$ seconds and can be found inFigure 2. The peak ground acceleration (PGA) recorded during this event was $0.84g$. The corresponding Fourier amplitude spectrum for the record is shown in Figure 3.

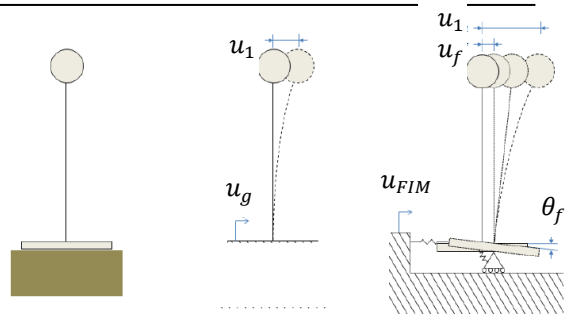

(a) Soil-Structure System (b) Fixed Base Model (c) Structural Model for Soil-Structure System

Figure 1. A simple soil-foundation-structure system with fixed base and sub-structure model[3].

Figure 1. Système sol-fondation-structure avec une base fixe et avec prise en compte de ISS [3].

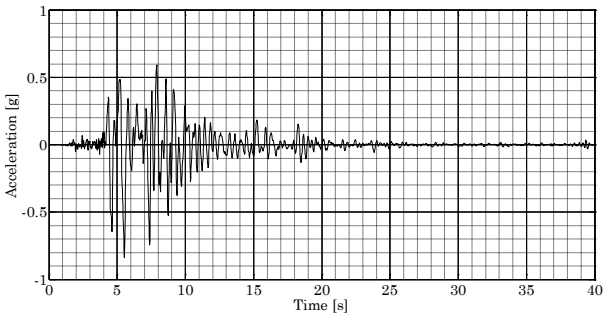

Figure 2. North-South ground acceleration recorded at the JMA survey during the January 17th, 1995, Kobe Earthquake.

Figure 2. Composante Nord-Sud de l'accélérogramme enregistrée lors du séisme de Kobe du 17 janvier 1995 à la station JMA.

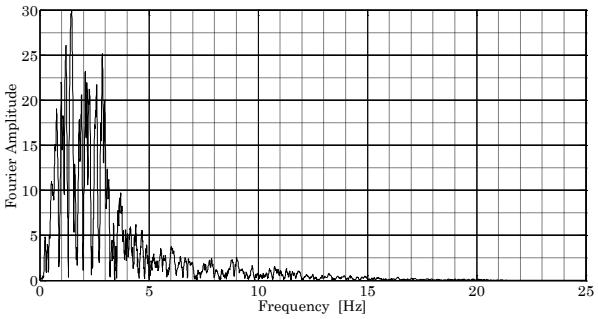

Figure 3. Fourier amplitude spectrum of North-South ground acceleration recorded on January 17th, 1995, Kobe Earthquake.

Figure 3. Composante Nord-Sud du spectre de Fourier de l'accélérogramme enregistré lors du séisme de Kobe du 17 janvier 1995.

The soil property values used in the following examples (see "Table 1") have been selected to reflect a typical soft soil in order to facilitate the interpretation of soil-structure interaction phenomena.

Table 1. Soil-Structure System Parameters.

		Soil		
G		Soil Bulk Modulus	68	MPa
	ρ	Mass Density	1.7	t/m3
VS		Shear Wave Velocity	200	m/s
	ν	Poisson's Ratio	0.45	-
		Structure		
	m	Structure mass	1200	Tons
	m_f	Foundation mass	250	Tons
h		Structure Height	12	m
T		Structural Period	0.4	Sec
	ξ	Critical damping Ratio	5	%
r		Foundation Radius	6.9	m
	h_t	Foundation Thickness	0.6	m

4.1-Set up of the differential equation of motion

Figure 1(b) shows a fixed-base model of the structure, where the soil is considered perfectly rigid. The system is excited by the selected free-field motion at the base, as shown inFigure 2. The acceleration of the ground motion, noted as u_g, represents the free-field motion or foundation input motion (*FIM*) (i.e., with no kinematic interaction effect), where $u_g = u_{FIM}$. The motion of the structure is governed by the following equation.

$$m\ddot{u}_n + c\dot{u}_n + ku_n = -m\,\ddot{u}_{g,n} \qquad (4)$$

where m, c, and k represent structural mass, damping, and stiffness and u_n, $\dot{u}_n$ and $\ddot{u}_n$ represents acceleration, velocity, and displacement at time n. On the right-hand-side of the equation, $u_{g,n}$represents the ground acceleration at time n. The system has a natural circular frequency of

$$\omega_0 = \sqrt{\frac{k}{m}} \qquad (5)$$

and a damping ratio

$$\xi = \frac{c}{2\sqrt{mk}} \qquad (6)$$

Noting that natural circular frequency is related to structural period by

$$\omega_0 = \frac{2\pi}{T} \qquad (7)$$

k and c may be expressed in terms of the values in The soil property values used in the following examples (see "Table 1") have been selected to reflect a typical soft soil in order to facilitate the interpretation of soil-structure interaction phenomena.
Table 1 as

$$k = \frac{4\pi^2 m}{T^2} \qquad (8)$$

and

$$c = 2\xi\sqrt{mk} \qquad (9)$$

with g representing gravitational acceleration.

Figure 1(c) shows a substructure model of the system. In this case, the rigid foundation is considered, however, the surrounding soil is replaced by the horizontal and rotational springs k_x, k_θ and dashpots c_x, c_θ, these latter are the foundation impedance function. Thus, the foundation is allowed to both translate and rotate (two additional degrees of freedom). As the system is relatively simple, a rigid disk foundation resting on a homogeneous soil half-space, suitable impedance functions are readily available in the literature. Veletsos and Verbic[7], define them as (Figure 4 and Figure 5)

$$\bar{k}_x = \frac{8Gr}{2-\nu}(k_x + ia_0c_x) \qquad (10)$$

Where

$$k_x = 1, \qquad c_x = 0.60 \qquad a_0 = \frac{\omega r}{V_s}$$

And

$$\bar{k}_\theta = \frac{8Gr^3}{3(1-\nu)}(k_\theta + ia_0c_\theta) \qquad (11)$$

Where

$$k_\theta = 1 - \frac{\beta_1(\beta_2 a_0)^2}{1+(\beta_2 a_0)^2} - \beta_3 a_0^2, c_\theta = \frac{\beta_1\beta_2(\beta_2 a_0)^2}{1+(\beta_2 a_0)^2},$$

$$\beta_1 = 0.8, \beta_2 = 0.45, \beta_3 = 0.023$$

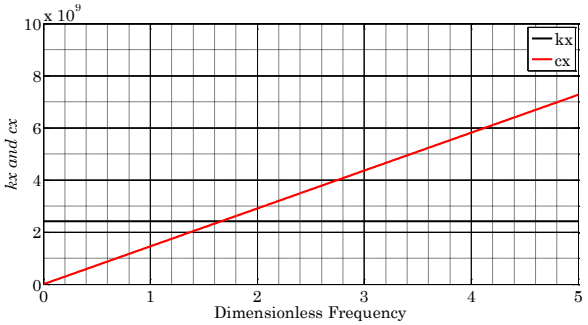

Figure 4. The horizontal component of the foundation impedance function stiffness and damping for disk resting on a homogeneous elastic half-space.

Figure 4. Composante horizontale de la fonction d'impédance (raideur et amortissement) pour un disque reposant sur une demi-espace élastique homogène.

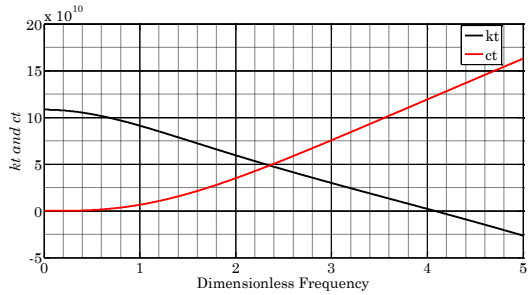

Figure 5. Therocking component of the foundation impedance function stiffness and damping for disk resting on a homogeneous elastic half-space.

Figure 5. Composante de balancement de la fonction d'impédance (raideur et amortissement) pour un disque reposant sur un demi-espace élastique homogène.

The soil-structure system is excited by the input motion of the foundation, which acts on the horizontal spring at its side. In the case of a fixed base model, both kinematic and inertial interactions are ignored. However, in the case of considering SSI, inertial interaction is considered, and the free-field motion is considered as the foundation input motion ($u_g = u_{FIM}$). This means that the kinematic interaction effect is neglected, which is only an assumption made in order to compare the results of both cases. Thus, the equations of motion for the soil-foundation-structure system may be written as follows:

$$\begin{bmatrix} m & 0 & 0 \\ 0 & m_f & 0 \\ 0 & 0 & I_f \end{bmatrix} \begin{Bmatrix} \ddot{u}_{1,n} \\ \ddot{u}_{f,n} \\ \ddot{\theta}_{f,n} \end{Bmatrix} + \begin{bmatrix} c & -c & -ch \\ -c & c & ch \\ -ch & ch & ch^2 \end{bmatrix} \begin{Bmatrix} \dot{u}_{1,n} \\ \dot{u}_{f,n} \\ \dot{\theta}_{f,n} \end{Bmatrix} + \begin{bmatrix} k & -k & -kh \\ -k & k & kh \\ -kh & kh & kh^2 \end{bmatrix} \begin{Bmatrix} u_{1,n} \\ u_{f,n} \\ \theta_{f,n} \end{Bmatrix} + \begin{Bmatrix} 0 \\ f_{x,n} \\ f_{\theta,n} \end{Bmatrix} = -\begin{Bmatrix} m \\ m_f \\ 0 \end{Bmatrix} \ddot{u}_{g,n} \quad (12)$$

In this equation, I_f represents the foundation's moment of inertia, h represents the structure's height, and $f_{x,n}$ and $f_{\theta,n}$ represent the forces generated by the impedance springs k_x and k_θ respectively. Starting in matrix form, these equations can be written as:

$$\boldsymbol{M}\ddot{u}_n + \boldsymbol{C}\dot{u}_n + \boldsymbol{K}u_n + \boldsymbol{f}_n = \boldsymbol{P}_n \quad (13)$$

with $\boldsymbol{M}$, $\boldsymbol{C}$, and $\boldsymbol{K}$ typically referred to as the system's mass, damping, and stiffness matrices.

As the foundation impedance functions vary with frequency, determination of f_n in the time domain is not evident. It is thus convenient to rewrite the equations of motion in the frequency domain as

$$\left(-\omega_l^2 \begin{bmatrix} m & 0 & 0 \\ 0 & m_f & 0 \\ 0 & 0 & I_f \end{bmatrix} + i\omega_l \begin{bmatrix} c & -c & -ch \\ -c & c & ch \\ -ch & ch & ch^2 \end{bmatrix} + \begin{bmatrix} k & -k & -kh \\ -k & k & kh \\ -kh & kh & kh^2 \end{bmatrix}\right) \begin{Bmatrix} U_{t,l} \\ U_{f,l} \\ \Theta_{f,l} \end{Bmatrix} + \begin{Bmatrix} 0 \\ F_{x,l} \\ F_{\theta,l} \end{Bmatrix} = -\begin{Bmatrix} m \\ m_f \\ 0 \end{Bmatrix} \ddot{U}_{g,l} \quad (14)$$

in which $U_{t,l}$, $U_{f,l}$, and $\Theta_{f,l}$ are the frequency domain representations of the displacements $u_{1,n}$, $u_{f,n}$, and $\theta_{f,n}$. The discrete Fourier transform must be used for conversion between the time and frequency domains. Thus

$$\ddot{U}_{g,l} = \mathcal{F}[\ddot{u}_{g,n}] \qquad (15)$$

where $\mathcal{F}[X]$indicate the discrete Fourier transform.

The forces generated by the impedance springs at each frequency value ω_l, represented by $F_{x,l}$and $F_{\theta,l}$, are thus calculated according to

$$F_{x,l} = \bar{k}_{x,l} U_{f,l} \text{and} F_{\theta,l} = \bar{k}_{\theta,l} \Theta_{f,l} \qquad (16)$$

Note that the subscript l in the Eq. (16) indicates that the original impedance functions $\bar{k}_{x,}$and $\bar{k}_{\theta}$ that have been sampled at L frequency points at a spacing of $\Delta\omega$. This convention is used to make a distinction between continuous impedance functions and sampled sequences of impedance data.

4.2-Fixed base response

First, the fixed-base model is considered, and the effects of inertial soil-structure interaction are ignored. During 1959, Newmark[38] proposed a numerical time-stepping integration scheme for solving differential equations such as the fixed-base equation of motion given in Eq. (4). This method remains widely used in engineering practice (Chopra,[39]). The obtained results from this simple model are still valuable to this study, as they can serve as a baseline from which to highlight the SSI effects.

"Figure 6" displays the fixed-base time-history response calculated using the Newmark method with β = 0.25 and γ = 0.5 for the system depicted in "Figure 1(a)", when excited by the horizontal ground acceleration depicted in "Figure 2". The response of the structure is calculated by two ways, 1) by the commercial software "SAP 2000" and 2) using "MATLAB" programs.

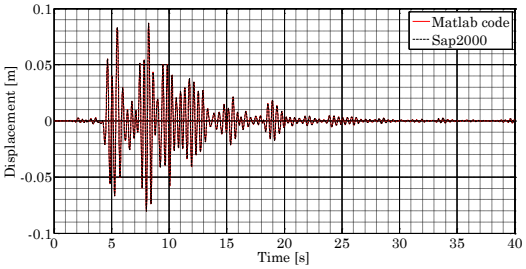

Figure 6. Fixed-base relative acceleration time-history response of SDOF structure subjected to horizontal ground acceleration.

Figure 6. Réponse temporelle en accélération relative pour le cas de la structure à base fixe sollicitée par une accélération horizontale.

The response results in a maximum horizontal displacement of $u_{max} = 8.70\ cm$. Analysis of the Fourier amplitude spectrum of the displacement response, as shown in Figure 7indicates a dominant period of $T_p = 0.40\ seconds$, which matches the period of the structure quite well. These fixed base values will serve as a baseline for the subsequent substructure analyses.

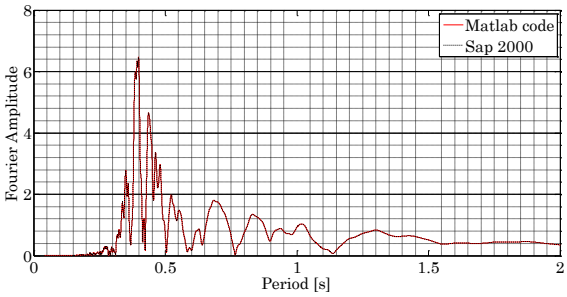

Figure 7. Fourier amplitude spectrum of fixed-base displacement time history for SDOF structure subjected to horizontal ground acceleration.

Figure 7. Spectre de Fourier de la variation temporelle du déplacement de la structure à base fixe sollicitée par une accélération horizontale.

4.3-Substructure frequency domain response

To determine the time-history response of the substructure model in the frequency domain, we begin by considering the force generated by the horizontal foundation impedance spring (according to Eq.(10), Eq.(11) and Eq.(16):

$$F_{x,l} = \bar{k}_{x,l} U_{f,l} = \frac{8Gr}{2-\nu}\left(k_{x,l} + i a_{0,l} c_{x,l}\right) U_{f,l} \quad (17)$$

$$\bar{F}_{\theta,l} = \bar{k}_{\theta,l} \Theta_{f,l} = \frac{8Gr^3}{3(1-\nu)}\left(k_{\theta,l} + i a_0 c_{\theta,l}\right) \Theta_{f,l} \quad (18)$$

For convenience, express this as

$$F_{x,l} = \left(\hat{k}_{x,l} + i\omega_l \hat{c}_{x,l}\right) U_{f,l} \quad (19)$$

And

$$F_{\theta,l} = \left(\hat{k}_{\theta,l} + i\omega_l \hat{c}_{\theta,l}\right) \Theta_{f,l} \quad (20)$$

Where

$$\hat{k}_{x,l} = k_{x,l}\frac{8Gr}{2-\nu} \qquad \hat{c}_{x,l} = c_{x,l}\frac{8Gr}{2-\nu}\frac{a_{0,l}}{\omega} \quad (21)$$

And

$$\hat{k}_{\theta,l} = k_{\theta,l}\frac{8Gr^3}{3(1-\nu)} \qquad \hat{c}_{\theta,l} = c_{\theta,l}\frac{8Gr^3}{3(1-\nu)}\frac{a_{0,l}}{\omega} \quad (22)$$

Substituting Eq.(19) and Eq.(20) into the equations of motion found in Eq.(12) yields.

$$\left(-\omega_l^2\begin{bmatrix} m & 0 & 0 \\ 0 & m_f & 0 \\ 0 & 0 & I_f \end{bmatrix} + i\omega_l\begin{bmatrix} c & -c & -ch \\ -c & c+\hat{c}_{x,l} & ch \\ -ch & ch & ch^2+\hat{c}_{\theta,l} \end{bmatrix} + \begin{bmatrix} k & -k & -kh \\ -k & k+\hat{k}_{x,l} & kh \\ -kh & kh & kh^2+\hat{k}_{\theta,l} \end{bmatrix}\right)\begin{Bmatrix} U_{t,l} \\ U_{f,l} \\ \Theta_{f,l} \end{Bmatrix} = -\begin{Bmatrix} m \\ m_f \\ 0 \end{Bmatrix}\ddot{U}_{g,l} \quad (23)$$

which may be expressed more compactly as

$$\left(-\omega^2 \boldsymbol{M} + i\omega\widetilde{\boldsymbol{C}} + \widetilde{\boldsymbol{K}}\right)\boldsymbol{U_l} = \boldsymbol{P}_l \quad (24)$$

where vectors $\boldsymbol{U_l}$ and $\boldsymbol{P_l}$ contain the system displacements and external forces at each frequency point l, and $\boldsymbol{M}$, $\widetilde{\boldsymbol{C}}$, and $\widetilde{\boldsymbol{K}}$ are referred to as the system's stiffness, damping and mass matrices. The tildes above the stiffness and damping matrices indicate that they include the frequency-dependent foundation impedance terms. Isolating $\boldsymbol{U}_l$ in Eq.(24) yields

$$\boldsymbol{U_l} = \boldsymbol{H}_l \boldsymbol{P}_l \quad (25)$$

in which the term

$$\boldsymbol{H_l} = \left(-\omega^2 \boldsymbol{M} + i\omega\widetilde{\boldsymbol{C}} + \widetilde{\boldsymbol{K}}\right)^{-1} \quad (26)$$

is typically referred to as the system's transfer function. Thus, determination of the system's displacement response requires multiplication of the external force vector by the system transfer function. The time history response may then be determined by converting the $\boldsymbol{U}_l$ into the time domain.“Figure 8” and “Figure 9” Shows respectively the amplitude and phase angle of the transfer function of the system. However, “Figure 10” shows the displacement time-history response for the substructure model depicted in “Figure 1(c)”, calculated using the frequency domain method outlined above. The figure highlights the effects of inertial SSI. In this figure, the solid line representing the SSI response reveals a maximum displacement of $\tilde{u}_{1,max}$= 14.65 cm calculate with MATLAB compared to a result calculated using Sap 2000. The effects of inertial SSI are also visible in the computed response’s Fourier amplitude spectrum, which is depicted in “Figure 11”. As expected, the response’s period lengthens, in this case from T_p = 0.40 seconds to $\tilde{T}_p \approx$ 0.48 seconds.

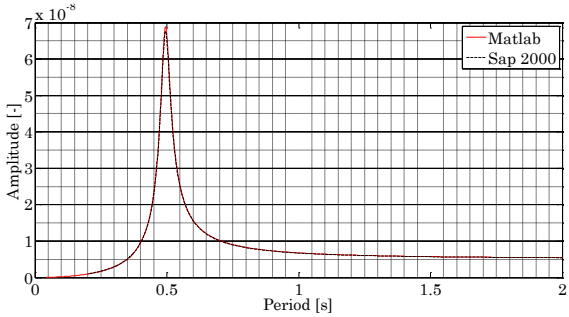

Figure 8. Amplitude of the transfer function of the soil-structure system.

Figure 8. Amplitude de la fonction de transfert du système sol-structure.

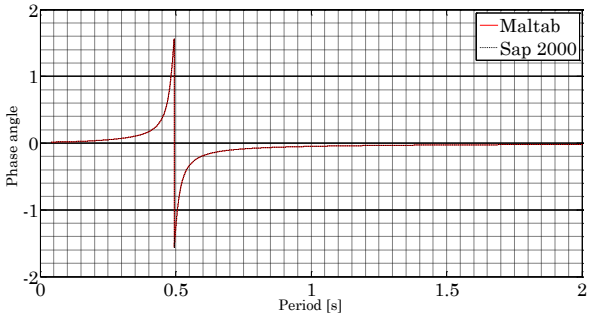

Figure 9. Phase of transfer function of the soil-structure system.

Figure 9. Phase de la fonction de transfert du système sol-structure.

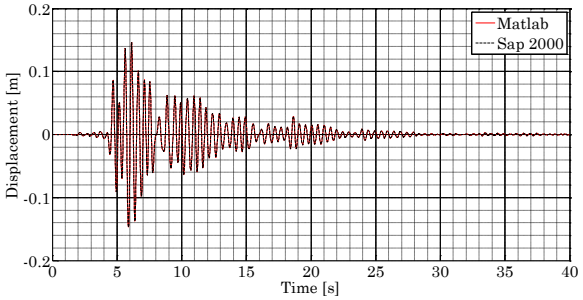

Figure 10. Displacement time-history response of the soil-structure system subjected to the ground acceleration (Substructure frequency domain response method).

Figure 10. Réponse temporelle en déplacement du système sol-structure sollicité par l'accélération horizontale du sol. (Méthode de réponse en domaine fréquentiel).

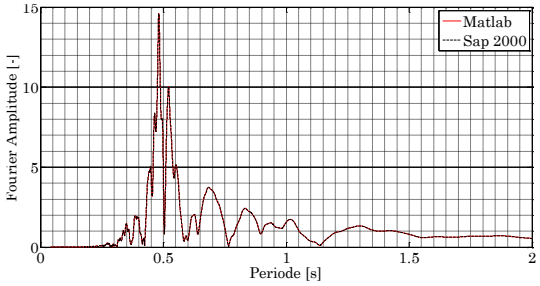

Figure 11. Fourier amplitude spectrum of the displacement time history for the soil-structure system subjected to the ground acceleration (Substructure frequency domain response method).

Figure 11. Spectre de Fourier de la variation temporelle du déplacement pour le système sol-structure sollicité par l'accélération du sol (méthode de sous-structure dans le domaine fréquentiel).

4.4-Substructure Representative Frequency Response

According to Gash[3], the most popular method currently used in practical engineering problems, in order to conduct the third step of the substructure method involves removing frequency dependence from the foundation impedance functions by evaluating them at some specific value of the frequency, this frequency is called representative frequency. Usually, this value is often taken as the structure's first mode flexible base natural frequency. It should be noted that this approach is currently adopted by the recommendationsNIST GCR 12-197-21[21]. In the case of the structure shown in Figure 1, the flexible-base period is evaluated as follows:

$$\tilde{T}_f = T\sqrt{1+\frac{k}{\bar{k}_{x,r}}+\frac{kh^2}{\bar{k}_{\theta,r}}} \qquad (27)$$

In Eq.(27), $\bar{k}_{x,r}$and $\bar{k}_{\theta,r}$ represent the specific value of $\bar{k}_x$and $\bar{k}_\theta$. As the former are frequency dependent. An alternative method, offered by Ghannad et al.[20], uses an eigenvalue analysis to determine the flexible-base period. For the system in "Figure 1c". Evaluating the foundation impedance functions at the frequency corresponding to this period yields scalar-valued impedances of $\bar{k}_{x,r}= 2.42\times10^9+i\,5.01\times10^7 N/m$ and $\bar{k}_{\theta,r} = 1.04\times10^{11}+i\,5.03\times10^7 N.m$. These values may be inserted into Eq.(12), leaving a set of equations of motions that are only dependent on time, and may be numerically integrated, using Newmark method, to determine the response of the system.

The representative frequency method results in a maximum displacement of $\tilde{u}_{1,max}$ = 15.9 cm and a predominant period of $\tilde{T}_p\approx$ 0.48 seconds, which closely match the values computed using the frequency domain. InFigure 12, the time history response of the structure is shown, calculated through two methods: 1) using the commercial software SAP 2000, and 2) utilizing MATLAB programs.

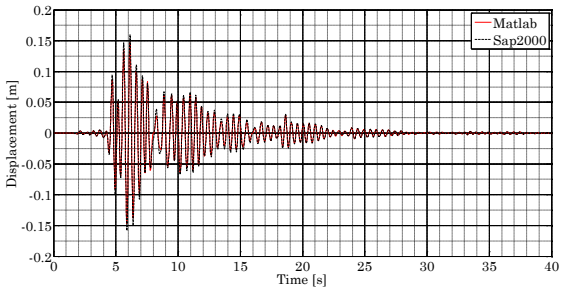

Figure 12. Displacement time-history response of the sol-structure system subjected to horizontal ground acceleration (representative frequency response method).

Figure 12. Réponse temporelle en déplacement du système sol-structure sollicité par l'accélération horizontale du sol. (Méthode de la réponse en fréquence représentative).

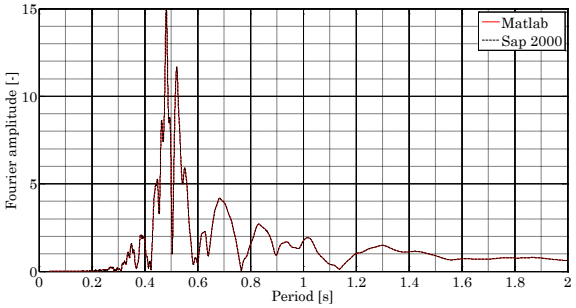

Figure 13. Fourier amplitude spectrum of the displacement time history for the soil-structure system subjected to the horizontal ground acceleration (substructure representative frequency response method.

Figure 13. Spectre de Fourier de la variation temporelle du déplacement pour le système sol-structure sollicité par l'accélération du sol (Méthode de la réponse en fréquence représentative).

4.5-Substructure lumped parameter model

Alternatively, to solve the equations of motion found in Eq.(12) by the method so called "substructure Lumped Parameter, (LP)" also known as, "the monkey tail—model". The presentation of the models is based on Wolf [10]for simple homogeneous half space. The most basic, or fundamental, lumped parameter model for horizontal and rocking motion is shown in "Figure 14".

The static stiffness are calculated using these equations:

$$k_{s,x} = \frac{8Gr}{2-\nu} \tag{28}$$

$$k_{s,\theta} = \frac{8Gr^3}{3-3\nu} \tag{29}$$

These are identical to the leading terms of Eq.(10) and Eq.(11) as Wolf used Veletsos and Verbic's impedance functions for his rigid disk on a homogeneous half-space formulation. The masses and dashpots are calculated according to

$$c_{0,j} = \frac{r}{V_S}\gamma_{0,j}k_{s,j} \tag{30}$$

$$c_{1,j} = \frac{r}{V_S}\gamma_{1,j}k_{s,j} \tag{31}$$

$$m_{0,j} = \frac{r^2}{V_S}\mu_{0,j}k_{s,j} \tag{32}$$

$$m_{1,j} = \frac{r^2}{V_S}\mu_{1,j}k_{s,j} \tag{33}$$

Where j represents the foundation displacement directions x or θ and the coefficients$\gamma_{0,j}$, $\gamma_{1,j}$, $\mu_{0,j}$, and $\mu_{1,j}$are calculated according to Table 2.

Table 2. Fundamental lumped parameter coefficients for rigid disk resting on uniform half-space.

Table 2. Coefficients fondamentaux des paramètres concentrés pour un disque rigide reposant sur un demi-espace uniforme.

j	$\gamma_{0,j}$	$\gamma_{1,j}$	$\mu_{0,j}$	$\mu_{1,j}$
x −Horizontal	$0.78 - 0.4\upsilon$	0	0	0
θ −Rocking	0	$0.42 - 0.3\upsilon^2$	0	$0.42 - 0.3\upsilon^2$

The set of equations of motion for the fundamental lumped parameter model corresponding to the system depicted in "Figure 1c" combined with system show in "Figure 14" is

$$\begin{bmatrix} m & 0 & 0 & 0 \\ 0 & m_{0,x}+m_f & 0 & 0 \\ 0 & 0 & m_{0,\theta} & 0 \\ 0 & 0 & 0 & m_{1,\theta} \end{bmatrix} \begin{Bmatrix} \ddot{u}_{t,n} \\ \ddot{u}_{f,n} \\ \ddot{\theta}_{f,n} \\ \ddot{\theta}_{1,n} \end{Bmatrix} + \begin{bmatrix} c & -c & -ch & 0 \\ -c & c+c_{0,x} & ch & 0 \\ -ch & ch & ch^2+c_{1,\theta} & -c_{1,\theta} \\ 0 & 0 & -c_{1,\theta} & c_{1,\theta} \end{bmatrix} \begin{Bmatrix} \dot{u}_{t,n} \\ \dot{u}_{f,n} \\ \dot{\theta}_{f,n} \\ \dot{\theta}_{1,n} \end{Bmatrix} + \begin{bmatrix} k & -k & -kh & 0 \\ -k & k+k_{s,x} & kh & 0 \\ -kh & kh & kh^2+k_{s,\theta} & 0 \\ 0 & 0 & 0 & 0 \end{bmatrix} \begin{Bmatrix} u_{t,n} \\ u_{f,n} \\ \theta_{f,n} \\ \theta_{1,n} \end{Bmatrix} = -\begin{Bmatrix} m \\ m_{0,x} \\ m_{0,\theta} \\ m_{1,\theta} \end{Bmatrix} \ddot{u}_{g,n} \quad (34)$$

By applying the system parameters from Table 2 and numerically integrating Eq. (40) with $\beta = 0.25$ and $\gamma = 0.5$, we obtained the response history. The lumped parameter model's approach produced a maximum displacement of $\tilde{u}_{1,max}$ = 15.70 cm and a predominant period of $\tilde{T}_p \approx 0.48$ seconds, which closely match the values calculated using the frequency domain. InFigure 15, we can see the time history response of the structure calculated using two methods: 1) the commercial software SAP 2000 and 2) MATLAB programs.

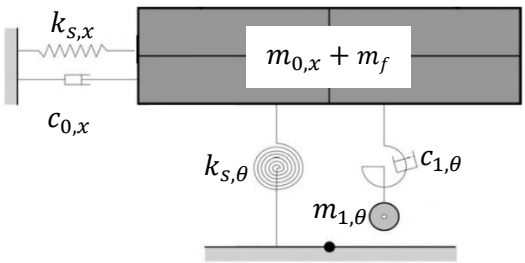

Figure 14. Fundamental lumped parameter model for horizontal and rockingmotion of rigid disk resting on a homogeneous elastic half-space.

Figure 14. Coefficients fondamentaux des paramètres concentréspour les composantes de translation et le balancementpour un disque rigide reposant sur un demi-espace uniforme.

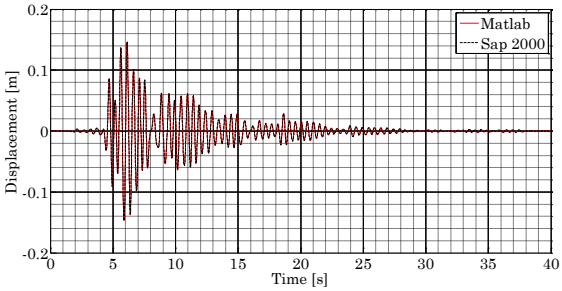

Figure 15. Displacement time-history response of the SSI system subjected to the foundation input motion (substructure lumped parameter mode method).

Figure 15. Réponse temporelle en déplacement du système sol-structure sollicité par l'accélération horizontale du sol.(méthode des coefficients fondamentaux des paramètres concentrés).

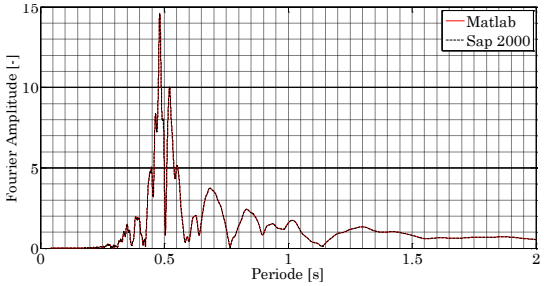

Figure 16. Fourier amplitude spectrum of the displacement time history for the SSI system subjected to the foundation input motion (substructure lumped parameter method).

Figure 16. Spectre de Fourier de la variation temporelle du déplacement pour le système sol-structure sollicité par l'accélération du sol(Coefficients fondamentaux des paramètres concentrés).

4.6-Substructure convolution

Substructure convolution is also a popular method which deals with the equations of motion found in Eq.(12). The process is conducted by executing a convolution between the impedance functions and the foundation displacements in the time domain. In order to explain the process, we consider only the horizontal component of the impedance function as an illustrative example. Expressing the foundation impedance function at each frequency step l as

$$\bar{k}_{x,l} = k_{x,l} + i\omega_l \hat{c}_{x,l} \quad (35)$$

Where, $\hat{c}_{x,l} = \frac{a_{0,l} c_{x,l}}{\omega_l}$
and ω represents frequency in (rad/s).

Therefore, the spring force generated by the foundation impedance function may be expressed in the frequency domain as

$$\bar{k}_{x,l}u_{x,l} = \left(k_{x,l} + i\omega_l \hat{c}_{x,l}\right)u_{x,l} \qquad (36)$$

As we are aware, a simple multiplication in the frequency domain is equivalent to a convolution integral in the time domain. So, Eq.(36) may be expressed in the time domain as

$$\bar{k}_{x,n} * u_{f,l} = k_{x,n} * u_{f,l} + \hat{c}_{x,n} * \dot{u}_{f,l} \qquad (37)$$

where $k_{x,n}$and $\hat{c}_{x,n}$represent the inverse discrete Fourier transforms, or impulse responses, of k_l and $\hat{c}_l$ respectively. This latter equation can be expressed by

$$\begin{aligned}\bar{k}_{x,n} * u_{f,l} = \\ k_{x,0}u_{f,n} + \sum_{j=1}^{n-1} k_{x,j}u_{f,n-j} + \hat{c}_{x,0}\dot{u}_{f,n} \\ + \sum_{j=1}^{n-1} \hat{c}_{x,j}\dot{u}_{f,n-j}\end{aligned} \qquad (38)$$

For a more compact writing, the zeroth term of both convolutions are expressed outside their respective summations as at every time step (n). When executing a numerical integration scheme to solve the equations of motion, displacements at all past time steps are known quantities. The force generated by the rotational impedance may then be substituted into Eq.(12) to yield the new version of the equations of motion:

$$\begin{aligned}&\begin{bmatrix} m & 0 & 0 \\ 0 & m_f & 0 \\ 0 & 0 & I_f \end{bmatrix}\begin{Bmatrix} \ddot{u}_{1,n} \\ \ddot{u}_{f,n} \\ \ddot{\theta}_{f,n} \end{Bmatrix} \\ &+\begin{bmatrix} c & -c & -ch \\ -c & c+\hat{c}_{x,0} & ch \\ -ch & ch & ch^2+\hat{c}_{\theta,0} \end{bmatrix}\begin{Bmatrix} \dot{u}_{1,n} \\ \dot{u}_{f,n} \\ \dot{\theta}_{f,n} \end{Bmatrix} \\ &+\begin{bmatrix} k & -k & -kh \\ -k & k+k_{x,0} & kh \\ -kh & kh & kh^2+k_{\theta,0} \end{bmatrix}\begin{Bmatrix} u_{1,n} \\ u_{f,n} \\ \theta_{f,n} \end{Bmatrix} \\ &= -\begin{Bmatrix} m \\ m_f \\ 0 \end{Bmatrix}\ddot{u}_{g,n} \\ &-\begin{Bmatrix} 0 \\ \sum_{j=1}^{n-1} k_{x,j}u_{f,n-j} + \hat{c}_{x,0}\dot{u}_{f,n} + \sum_{j=1}^{n-1} \hat{c}_{x,j}\dot{u}_{f,n-j} \\ \sum_{j=1}^{n-1} k_{x,j}\theta_{f,n-j} + \hat{c}_{x,0}\dot{u}_{f,n} + \sum_{j=1}^{n-1} \hat{c}_{x,j}\dot{\theta}_{f,n-j} \end{Bmatrix}\end{aligned} \qquad (39)$$

The unknown displacement terms at time step n are grouped on the left-hand side inside the structural stiffness and damping matrices, while the known terms at time steps $n-l$ are grouped on the right-hand side. With this arrangement, the equations of motion can be solved using Newmark's numerical integration technique.

Although the current method appears to be suitable for the problem, it suffers from stability issues due to limitations in the frequency range of the impedance function. The inverse Fourier transform requires knowledge of all data over the frequency interval $(-\infty \le \omega \le \infty)$, but impedance functions are often evaluated for limited frequency intervals, such as $0 \le a_0 \le 5$. The use of truncated or conditioned inverse discrete Fourier transforms can lead to non-causal results, where the current displacement depends on both past and future displacements. To be usable with time-stepping numerical integration schemes, non-causal responses must be adjusted to be causal.

Various methods have been proposed to address this issue. Some methods involve conditioning the inverse discrete Fourier transform(IDFT), such as those proposed by Paronesso and Wolf [34] or Hayashi and Katukura[29]. Other methods use curve-fitting techniques, such as the method proposed by Nakamura[30], which avoids the IDFT altogether. Gash [3] uses a modified version of an iterative technique borrowed from the signal processing community to enforce causality and adjust time domain parameters based on band-limited frequency domain data. This method is based on the method developed by Luo and Chen [40], which involves successive iterations of the IDFT and discrete Fourier transform (DFT) over a frequency range extended beyond the original frequency data range, with causality enforced during each iteration. The iterations terminate when the DFT of the impulse response of the adjusted data is within a desired tolerance of the original frequency data over the original range of interest.

The original method by Luo and Chen is modified here because the impulse responses in Eq.(37) are generated from real, as opposed to complex, data. To demonstrate the correction technique, consider the case of a notional band limited data sequence Y_l. Assume this sequence contains real-valued data at discrete frequencies l from zero to some cutoff frequency ω_c, after which it assumes zero values up to a maximum

frequency of ω_L. Begin by applying the IDFT to compute the sequence's impulse response:

$$y_n = \mathcal{F}^{-1}[Y_l] \quad (40)$$

Next, compute a causal approximation of this impulse response by setting all values occurring at negative time steps to zero according to:

$$\hat{y}_n = y_n \mathcal{H}_n \quad (41)$$

where, $\mathcal{H}_n$ is a Heaviside function defined as

$$\mathcal{H}_n = \begin{cases} 0 \ \ if \ \ n < 0 \\ \\ 1 \ \ if \ \ n \geq 0 \end{cases} \quad (42)$$

Then transform this causal approximation back into the frequency domain using the DFT to yield an approximation of the original sequence Y_l,

$$\hat{Y}_l = \mathcal{F}[\hat{y}_n] \quad (43)$$

Next, compute the difference between theoriginal sequence and approximation:

$$\bar{k}_{x,n} * u_{f,l} = k_{x,n} * u_{f,l} + \hat{c}_{x,n} * u_{f,l} \quad (44)$$

Use this difference to determine the maximum absolute error between the original sequence and the approximation over the original frequency range of interest ($0 \leq l \leq \omega_c$)

$$\Delta Y_l = Y_l - \hat{Y}_l \quad (45)$$

If ε is within a desired tolerance, then $\hat{y}_n$ is the desired causal time domain impulse response. If not, then a correction is applied to$\hat{Y}_l$. Note that this correction is applied differently for values of $\hat{Y}_l$ inside and outside the original frequency band of interest. Inside the band of interest, the correction is

$$\hat{Y}_l = \hat{Y}_l - \Delta\hat{Y}_l \quad (46)$$

Where

$$\Delta\hat{Y}_l = \alpha_k \, \Delta Y_l \quad (47)$$

and α is a weight factor computed during each iteration as

$$\alpha = \alpha - \varepsilon \quad (48)$$

with a seed value of $\alpha = 1$. Outside the frequency range of interest ($\omega_c < l \leq \omega_L$), the correction is

$$\bar{k}_{x,n} * u_{f,l} = k_{x,n} * u_{f,l} + \hat{c}_{x,n} * u_{f,l} \quad (49)$$

with the constant 0.99 selected to both damp $\hat{Y}_l$as l approaches L and to assure a smooth transition from inside to outside the frequency range of interest.

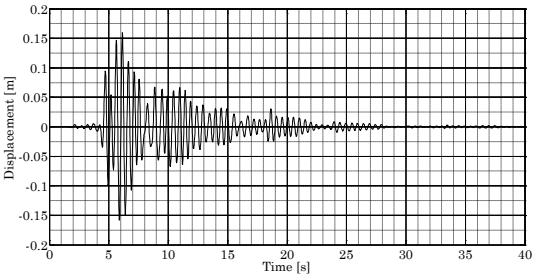

Figure 17. Displacement time-history response of the soil-structure system subjected to the foundation input motion (substructure convolution method).

Figure 17. Réponse temporelle en déplacement du système sol-structure sollicité par l'accélération horizontale du sol (méthode de convolution).

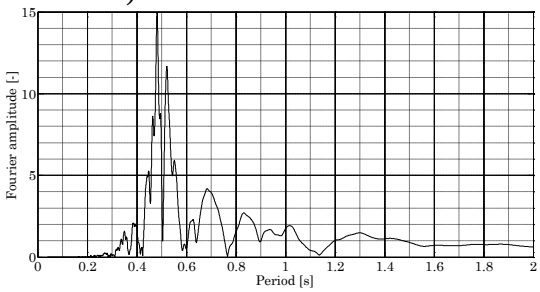

Figure 18. Fourier amplitude spectrum of the displacement time history for the soil-structure system subjected to the foundation input motion (convolution).

Figure 18. Spectre de Fourier de la variation temporelle du déplacement pour le système sol-structure sollicité par l'accélération du sol (méthode de convolution).

The substructure convolution method yields a maximum displacement of $\tilde{u}_{1,max}$ = 15.75 cm and a predominant period of $\tilde{T} \approx$ 0.48 seconds, which closely match the values computed using the frequency domain. For this method, it is practically not possible to perform calculations using this method using commercially available convolutional software. Since the calculation process is based on the force vector actualization for each time step, which requires specific programming in open-source software.

4.7-Substructure filter method

In this section, the formulation of filter method based on Safak's idea is presented. For more details, the reader can refer to Şafak[37], Gash [3] and Gash et al.[41]. So, Safak's idea was to use signal processing theory to approximate the spring force generated by impedance functions as discrete-time digital filters. Such filters are essentially mathematical tools that convert inputs into desired outputs. Safak proposed using present and past values of foundation displacement, coupled with past values of spring force as the inputs to predict, as output, the current value of force generated by the impedance function. Accordingly, in the time domain, the spring force generated in the impedance function k_n can be written as:

$$\begin{aligned}\bar{k}_n * u_{f,n} \approx f_n = {} & b_0 u_{f,n} + b_1 u_{f,n-1} \\ & + \cdots + b_j u_{f,n-j} \\ & - a_1 f_{,n-1} + \cdots \\ & + a_j f_{,n-j}\end{aligned} \tag{50}$$

$$\begin{aligned}\bar{k}_n * u_{f,n} \approx f_n = {} & b_0 u_{f,n} \\ & + \sum_{j=1}^{J} b_p u_{f,n-j} \\ & + \sum_{j=1}^{J} b_q u_{f,n-j}\end{aligned} \tag{51}$$

where J represents the filter order. Note the similarity between these relations and those for the convolution solution given in Eq.(37) and Eq.(38). The Eq. (51) may be inserted in a similar manner into a numerical integration scheme, such as Eq.39, and used to conduct time-history analyses in the time domain in a manner similar to that employed for the convolution solution.

Recall the soil-foundation-structure system shown in Figure 1c. The equations of motion for the substructure model of this system, also given in Eq.(12), are

$$\begin{aligned}&\begin{bmatrix} m & 0 & 0 \\ 0 & m_f & 0 \\ 0 & 0 & I_f \end{bmatrix} \begin{Bmatrix} \ddot{u}_{1,n} \\ \ddot{u}_{f,n} \\ \ddot{\theta}_{f,n} \end{Bmatrix} + \\ &\begin{bmatrix} c & -c & -ch \\ -c & c & ch \\ -ch & ch & ch^2 \end{bmatrix} \begin{Bmatrix} \dot{u}_{1,n} \\ \dot{u}_{f,n} \\ \dot{\theta}_{f,n} \end{Bmatrix} + \\ &\begin{bmatrix} k & -k & -kh \\ -k & k & kh \\ -kh & kh & kh^2 \end{bmatrix} \begin{Bmatrix} u_{1,n} \\ u_{f,n} \\ \theta_{f,n} \end{Bmatrix} + \begin{Bmatrix} 0 \\ f_{x,n} \\ f_{\theta,n} \end{Bmatrix} \\ &= -\begin{Bmatrix} m \\ m_f \\ 0 \end{Bmatrix} \ddot{u}_{g,n}\end{aligned} \tag{52}$$

From the Eq.(51), the spring force generated by the horizontal and rocking foundation impedance functions take the form

$$\begin{aligned}f_{x,n} = {} & b_{x,0} u_{f,n} + \sum_{j=1}^{J} b_{x,p} u_{f,n-j} \\ & + \sum_{j=1}^{J} b_{x,q} u_{f,n-j}\end{aligned} \tag{53}$$

for the horizontal direction and

$$\begin{aligned}f_{\theta,n} = {} & b_{\theta,0} u_{f,n} + \sum_{j=1}^{J} b_{\theta,p} u_{f,n-j} \\ & + \sum_{j=1}^{J} b_{\theta,q} u_{f,n-j}\end{aligned} \tag{54}$$

for the rocking direction. When conducting a time-history analysis using numerical integration, past values of the foundation displacements u_f and θ_f and the spring forces f_f and f_θ are known quantities. Given this, substituting Eq.(54) and Eq.(53) into Eq.(52) and grouping these known values on the right-hand side of the resulting equations yields

$$\begin{bmatrix} m & 0 & 0 \\ 0 & m_f & 0 \\ 0 & 0 & I_f \end{bmatrix} \begin{Bmatrix} \ddot{u}_{1,n} \\ \ddot{u}_{f,n} \\ \ddot{\theta}_{f,n} \end{Bmatrix} + \begin{bmatrix} c & -c & -ch \\ -c & c & ch \\ -ch & ch & ch^2 \end{bmatrix} \begin{Bmatrix} \dot{u}_{1,n} \\ \dot{u}_{f,n} \\ \dot{\theta}_{f,n} \end{Bmatrix} + \begin{bmatrix} k & -k & -kh \\ -k & k+b_{x,0} & kh \\ -kh & kh & kh^2+b_{\theta,0} \end{bmatrix} \begin{Bmatrix} u_{1,n} \\ u_{f,n} \\ \theta_{f,n} \end{Bmatrix} = -\begin{Bmatrix} m \\ m_f \\ 0 \end{Bmatrix} \ddot{u}_{g,n} + \begin{Bmatrix} 0 \\ \hat{f}_{x,n} \\ \hat{f}_{\theta,n} \end{Bmatrix} \quad (55)$$

Where

$$\hat{f}_{x,n} = \sum_{p=1}^{P} b_{x,p} u_{f,n-p} + \sum_{q=1}^{Q} b_{x,q} u_{f,n-q} \quad (56)$$

$$\hat{f}_{\theta,n} = \sum_{p=1}^{P} b_{x,p} u_{f,n-p} + \sum_{q=1}^{Q} b_{x,q} u_{f,n-q} \quad (57)$$

Stated in matrix from, these equations of motion become:

$$\boldsymbol{M}\ddot{\boldsymbol{u}}_n + \boldsymbol{C}\dot{\boldsymbol{u}}_n + \hat{\boldsymbol{K}}\boldsymbol{u}_n = \hat{\boldsymbol{P}}_{\boldsymbol{n}} \quad (58)$$

Where, $\boldsymbol{M}$is the system mass matrix, $\boldsymbol{C}$ is the system damping matrix. The filter adjusted stiffness matrix and force are $\hat{\boldsymbol{K}}$ and $\hat{\boldsymbol{P}}_{\boldsymbol{n}}$ respectively and the acceleration, velocity, and displacement vectors are likewise $\ddot{\boldsymbol{u}}_n$, $\dot{\boldsymbol{u}}_n$, and $\boldsymbol{u}_n$.
Using these equations of motion, the system's time-history response may now be determined through application of Newmark's numerical time-stepping integration method in a manner like the previous examples.

Table 3. Coefficients of discrete-time filters approximating horizontal and rocking impedance functions for rigid disk resting on uniform soil half-space.
Table 3. Coefficients des filtres récursifs approximant les fonctions d'impédance horizontale et de balancement pour un disque rigide reposant sur un demi-espace de sol uniforme.

j	$a_{x,j}$	$b_{x,j} \times 10^{11}$	$a_{\theta,j}$	$b_{\theta,j} \times 10^{8}$
1	1	0.0743	1.0000	0.0743
2	28.0772	1.9872	28.0772	1.9872
3	27.0772	-0.7016	27.0772	-0.7016

To demonstrate the procedure, once again recall the system depicted in "Figure 1c" theaccompanying values listed in The soil property values used in the following examples (see "Table 1") have been selected to reflect a typical soft soil in order to facilitate the interpretation of soil-structure interaction phenomena.
Table 1, and the input ground motion shown in Figure 2.

Applying the algorithm to the horizontal impedance function yields the second order filter coefficients. The magnitude and phase components of both the original impedance function and the filter approximation are shown in Figure 19 and Figure 20. The fit is quite good across the entire frequency range. It should be noted that the least-squares algorithm returned a negligible imaginary component for each coefficient, thus producing what is, in essence, a real filter.

Applying this yields the fourth order filter coefficients also found in Table 3. The original rocking impedance function and the filter approximation are shown in Figure 20. Notice that while the fit is generally good over the lower two-thirds of the frequency domain it deteriorates significantly in the upper third, beginning at around 19 Hertz.

Fortunately, recalling Figure 19, nearly all of the input motion's frequency content is found below this threshold with the majority occurring from 0 to 25 Hertz.

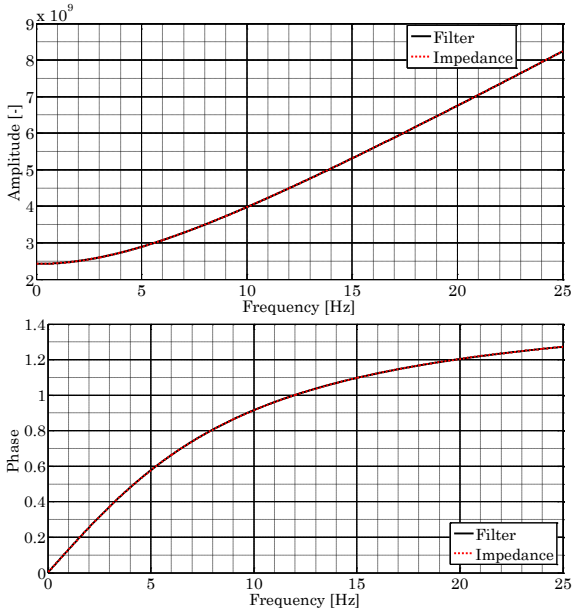

Figure 19. Comparison of foundation impedance function and filter approximation for rigid disk resting on a homogeneous soil half-space.(Horizontal component)

Figure 19. Comparaison de la fonction d'impédance de fondation et de l'approximation par filtre récursif pour un disque rigide reposant sur un demi-espace de sol homogène. (Composante horizontale)

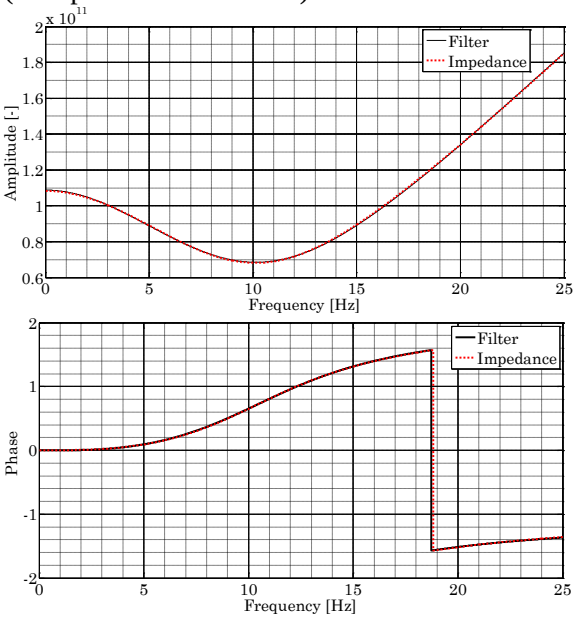

Figure 20. Comparison of rocking foundation impedance function and filter approximation for rigid disk resting on a homogeneous soil half-space.(Rocking component)

Figure 20. Comparaison de la fonction d'impédance de fondation et de l'approximation par filtre récursif pour un disque rigide reposant sur un demi-espace de sol homogène. (Composante de balancement)

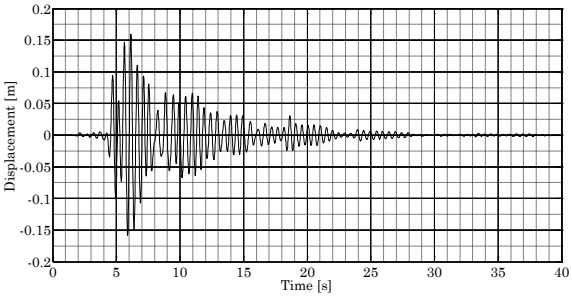

Figure 21. Displacement time-history response of the soil-structure system subjected to horizontal ground acceleration (filter method).

Figure 21. Réponse temporelle en déplacement du système sol-structure sollicité par l'accélération horizontale du sol (méthode des filtres récursifs).

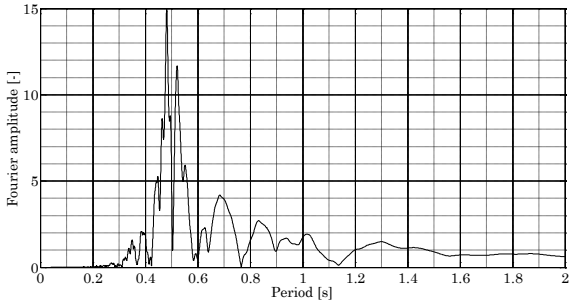

Figure 22. Fourier amplitude spectrum of the displacement time history for the soil-structure system subjected to the horizontal ground acceleration (filter method).

Figure 22 Spectre de Fourier de la variation temporelle du déplacement pour le système sol-structure sollicité par l'accélération du sol (méthode des filtres récursifs).

The substructure filter method yields a maximum displacement of $\tilde{u}_{1,max}$= 15.72 cm and a predominant period of T̃ = 0.48 seconds, which closely match the values computed using the frequency domain. Figure 21 shows the time history response of the structure calculated using MATLAB programs. As pointed out in the previous method (convolution method), it is not practical to perform calculations using commercially available convolutional software. Since the calculation process is based on the force vector actualization for each time step, specific programming is required in open-source software.

5-Comparison of Methods

We present in the following the principles calculation results obtained in the previous sections. Table 4 summarizes the results of the calculations derived from the different methods and their application field. However,Figure 23 and Figure 24 present respectively a comparison between the time history and Fourier amplitude spectrum of the displacement response obtained by different methods.

Table 4. Comparison of the time response results of the soil-structure system obtained by different methods with the response of the fixed-base structure.

Table 4. Comparaison des résultats de réponse temporelle du système sol-structure obtenus par différentes méthodes avec la réponse de la structure à base fixe.

Model	Period [S]	Max. Structural Displacement [cm]	Model
Fixed-Base	0.4	8.7	Linear and nonlinear
Frequency Domain	0.48	15.6	Linear only
Representative Frequency	0.48	15.9	Linear only
Lumped Parameter	0.48	15.70	Linear and nonlinear
Corrected Convolution	0.48	15.75	Linear and nonlinear
Filter Method	0.48	15.72	Linear and nonlinear

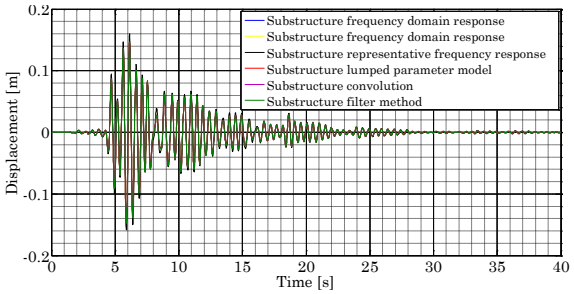

Figure 23. Comparison of displacement time-history response of the soil-structure system calculated by different methods.

Figure 23. Comparaison de la réponse temporelle de déplacement du système sol-structure calculée par différentes méthodes.

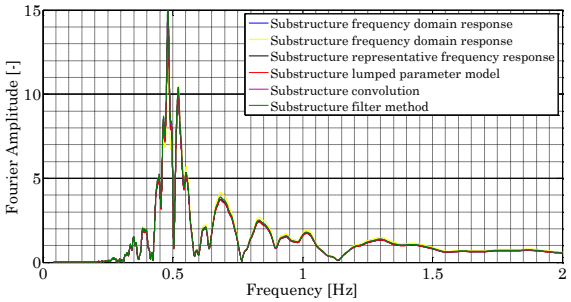

Figure 24. Fourier amplitude spectrum of the displacement time history for the soil structure system calculated by different methods.

Figure24. Spectre de Fourier de la variation temporelle du déplacement pour le système sol-structure calculée par différentes méthodes.

6-Conclusion

This research paper aimed to explore the current practices employed for dealing with the frequency dependence of impedance functions through the substructure approach. To achieve this, five distinct approaches were presented and examined with a numerical example that illustrated their effectiveness. The study showed that all substructure methods produced similar results to the fixed base predominant period and maximum structural displacement. However, it is important to note that these methods were tested on a linear superstructure, which is suitable for all five approaches. For nonlinear superstructures, only three methods were found to be applicable: the Convolution method, Filter method, and Lumped Parameters method. Among these methods, only the Lumped Parameters method can be directly integrated with commercial finite element software for more advanced modeling. The Filter method and Convolution method require open-source software and further implementation.

In conclusion, this research study showed that the substructure approach is an effective way of dealing with the frequency dependence of impedance functions.

Référencesbibliographiques

[1] E. Kausel, “Early history of soil–structure interaction,” Soil Dynamics and Earthquake Engineering, vol. 30, no. 9, pp. 822–832, Sep. 2010, doi: 10.1016/j.soildyn.2009.11.001.

[2] J. M. Roesset, “Soil Structure Interaction The Early Stages,” Journal of Applied Science and Engineering, vol. 16, no. 1, pp. 1–8, Mar. 2013, doi: 10.6180/jase.2013.16.1.01.

[3] R. J. H. Gash, A. H. Sayed, J. P. Stewart, and J. Zhang, “Title: On the Implementation and Applications of Discrete-Time Filters for Soil-Structure Interaction Analyses.” [Online]. Available: http://escholarship.org/uc/item/9vv3g5gzhttp://www.escholarship.org/help_copyright.html#reuse

[4] J. Zhang and Y. Tang, “Dimensional analysis of structures with translating and rocking foundations under near-fault ground motions,” Soil Dynamics and Earthquake Engineering, vol. 29, no. 10, pp. 1330–1346, Oct. 2009, doi: 10.1016/J.SOILDYN.2009.04.002.

[5] Kausel, “Forced vibrations of circular foundations on layered media. Research report,” 1974.

[6] A. S. Veletsos and Y. T. Wei, “Lateral and Rocking Vibration of Footings,” Journal of the Soil Mechanics and Foundations Division, vol. 97, no. 9, pp. 1227–1248, Sep. 1971, doi: 10.1061/JSFEAQ.0001661.

[7] A. S. Veletsos and B. Verbič, “Vibration of viscoelastic foundations,” Earthq Eng Struct Dyn, vol. 2, no. 1, pp. 87–102, 1973, doi: 10.1002/eqe.4290020108.

[8] G. Gazetas, “Foundation Vibrations,” in Foundation Engineering Handbook, Boston, MA: Springer US, 1991, pp. 553–593. doi: 10.1007/978-1-4615-3928-5_15.

[9] M. Novak, “Effect of soil on structural response to wind and earthquake,” Earthq Eng Struct Dyn, vol. 3, no. 1, pp. 79–96, 1974, doi: 10.1002/eqe.4290030107.

[10] J. P. Wolf, Foundation vibration analysis using simple physical models. Pearson Education, 1994.

[11] J. P. Wolf and A. J. Deeks, Foundation Vibration Analysis: A Strength-of-materials Approach. Elsevier, 2004. [Online]. Available: https://books.google.dz/books?id=1nAamAEACAAJ

[12] J. Lysmer and R. L. Kuhlemeyer, “Finite Dynamic Model for Infinite Media,” Journal of the Engineering Mechanics Division, vol. 95, no. 4, pp. 859–877, Aug. 1969, doi: 10.1061/JMCEA3.0001144.

[13] R. J. Apsel and J. E. Luco, "Impedance functions for foundations embedded in a layered medium: An integral equation approach," Earthq Eng Struct Dyn, vol. 15, no. 2, pp. 213–231, Feb. 1987, doi: 10.1002/eqe.4290150205.

[14] C. C. Spyrakos and C. Xu, "Dynamic analysis of flexible massive strip–foundations embedded in layered soils by hybrid BEM–FEM," Comput Struct, vol. 82, no. 29–30, pp. 2541–2550, Nov. 2004, doi: 10.1016/j.compstruc.2004.05.002.

[15] Z. Han, G. Lin, and J. Li, "Dynamic Impedance Functions for Arbitrary-Shaped Rigid Foundation Embedded in Anisotropic Multilayered Soil," J Eng Mech, vol. 141, no. 11, Nov. 2015, doi: 10.1061/(ASCE)EM.1943-7889.0000915.

[16] R. Bencharif, M. Hadid, and N. Mezouar, "Hybrid BEM-TLM-PML method for the dynamic impedance functions calculation of a rigid strip-footing on a nearly saturated poroelastic soil profile," Eng Anal Bound Elem, vol. 116, pp. 31–47, Jul. 2020, doi: 10.1016/j.enganabound.2020.03.001.

[17] R. Bencharif, "Non-linear soil-structure interaction analysis based on a substructure method incorporating an approximate 3D approach," Master, Building Research Institute, BRI, Tsukuba, 2017.

[18] R. W. Clough and J. Penzien, Dynamics of Structures. in International student edition. McGraw-Hill, 1975. [Online]. Available: https://books.google.dz/books?id=2VwbtAEACAAJ

[19] A. Duarte Laudon, O.-S. Kwon, and A. R. Ghaemmaghami, "Stability of the time-domain analysis method including a frequency-dependent soil-foundation system," Earthq Eng Struct Dyn, vol. 44, no. 15, pp. 2737–2754, Dec. 2015, doi: 10.1002/eqe.2606.

[20] G. M. Ali, "11 A STUDY ON THE FREQUENCY AND DAMPING OF SOIL-STRUCTURE SYSTEMS USING A SIMPLIFIED MODEL," 構造工学論文集. B, no. 44, pp. 85–93, 1998.

[21] N. Gcr, "Soil-Structure Interaction for Building Structures," National Institute of Standards and Technology (NEHRP), 2012.

[22] W.-H. Wu and W.-H. Lee, "Systematic lumped-parameter models for foundations based on polynomial-fraction approximation," Earthq Eng Struct Dyn, vol. 31, no. 7, pp. 1383–1412, Jul. 2002, doi: 10.1002/eqe.168.

[23] A. Zahafi and M. Hadid, "Simplified frequency-independent model for vertical vibrations of surface circular foundations," World Journal of Engineering, vol. 16, no. 5, pp. 592–603, Oct. 2019, doi: 10.1108/WJE-05-2019-0145.

[24] A. Zahafi, M. Hadid, and R. Bencharif, "Lumped parameter model for vertical vibrations of surface circular foundations on nonhomogeneous soil," World Journal of Engineering, vol. ahead-of-print, no. ahead-of-print, Jan. 2023, doi: 10.1108/WJE-01-2023-0012.

[25] J. P. Wolf and P. Obernhuber, "Non-linear soil-structure-interaction analysis using dynamic stiffness or flexibility of soil in the time domain," Earthq Eng Struct Dyn, vol. 13, no. 2, pp. 195–212, Mar. 1985, doi: 10.1002/eqe.4290130205.

[26] J. P. Wolf and M. Motosaka, "Recursive evaluation of interaction forces of unbounded soil in the time domain," Earthq Eng Struct Dyn, vol. 18, no. 3, pp. 345–363, Apr. 1989, doi: 10.1002/eqe.4290180304.

[27] J. W. Meek, "Recursive analysis of dynamic phenomena in civil engineering," Bautechnik, vol. 67, pp. 205–210, 1990.

[28] M. Motosaka and M. Nagano, "Recursive evaluation of convolution integral in nonlinear soil-structure interaction analysis and its applications," Journal of Structural and Construction Engineering (AIJ), vol. 436, pp. 71–80, 1992.

[29] Y. Hayashi and H. Katukura, "Effective time-domain soil-structure interaction analysis based on FFT algorithm with causality condition," Earthq Eng Struct Dyn, vol. 19, no. 5, pp. 693–708, Jul. 1990, doi: 10.1002/eqe.4290190506.

[30] N. Nakamura, "A practical method to transform frequency dependent impedance to time domain," Earthq Eng Struct Dyn, vol. 35, no. 2, pp. 217–231, Feb. 2006, doi: 10.1002/eqe.520.

[31] N. Nakamura, "Improved methods to transform frequency-dependent complex stiffness to time domain," Earthq Eng Struct Dyn, vol. 35, no. 8, pp. 1037–1050, Jul. 2006, doi: 10.1002/eqe.570.

[32] N. Nakamura, "Transform methods for frequency-dependent complex stiffness to time domain using real or imaginary data only," Earthq Eng Struct Dyn, vol. 37, no. 4, pp. 495–515, Apr. 2008, doi: 10.1002/eqe.767.

[33] N. Nakamura, "Nonlinear Response Analysis Considering Dynamic Stiffness with Both Frequency and Strain Dependencies," J Eng Mech, vol. 134, no. 7, pp. 530–541, Jul. 2008, doi: 10.1061/(ASCE)0733-9399(2008)134:7(530).

[34] A. Paronesso and J. P. Wolf, "Global lumped-parameter model with physical representation for unbounded medium," Earthq Eng Struct Dyn, vol. 24, no. 5, pp. 637–654, May 1995, doi: 10.1002/eqe.4290240503.

[35] P. Ruge, C. Trinks, and S. Witte, "Time-domain analysis of unbounded media using mixed-variable formulations," Earthq Eng Struct Dyn, vol. 30, no. 6, pp. 899–925, Jun. 2001, doi: 10.1002/eqe.47.

[36] X. Du and M. Zhao, "Stability and identification for rational approximation of frequency response function of unbounded soil," Earthq Eng Struct Dyn, p. n/a-n/a, 2009, doi: 10.1002/eqe.936.

[37] E. Şafak, "Time-domain representation of frequency-dependent foundation impedance functions," Soil Dynamics and Earthquake Engineering, vol. 26, no. 1, pp. 65–70, Jan. 2006, doi: 10.1016/j.soildyn.2005.08.004.

[38] N. M. Newmark, "A Method of Computation for Structural Dynamics," Journal of the Engineering Mechanics Division, vol. 85, no. 3, pp. 67–94, Jul. 1959, doi: 10.1061/JMCEA3.0000098.

[39] A. K. Chopra, Dynamics of Structures. in Prentice-Hall international series in civil engineering and engineering mechanics. Pearson Education, 2007. [Online]. Available: https://books.google.dz/books?id=0dU1bDaRyP4C

[40] Shuiping Luo and Zhizhang Chen, "Iterative methods for extracting causal time-domain parameters," IEEE Trans Microw Theory Tech, vol. 53, no. 3, pp. 969–976, Mar. 2005, doi: 10.1109/TMTT.2004.842480.

[41] R. Gash, E. EsmaeilzadehSeylabi, and E. Taciroglu, "Implementation and stability analysis of discrete-time filters for approximating frequency-dependent impedance functions in the time domain," Soil Dynamics and Earthquake Engineering, vol. 94, pp. 223–233, Mar. 2017, doi: 10.1016/j.soildyn.2017.01.021.